Hypofractionated FLASH-RT as an Effective Treatment against Glioblastoma that Reduces Neurocognitive Side Effects in Mice ⒶⒸ

Pierre Montay-Gruel[1], Munjal M. Acharya[2], Patrik Gonçalves Jorge[1,3], Benoît Petit[1], Ioannis G. Petridis[1], Philippe Fuchs[1], Ron Leavitt[1], Kristoffer Petersson[1,3], Maude Gondré[1,3], Jonathan Ollivier[1], Raphael Moeckli[3], François Bochud[3], Claude Bailat[3], Jean Bourhis[1], Jean-François Germond[3], Charles L. Limoli[2], and Marie-Catherine Vozenin[1]

ABSTRACT

Purpose: Recent data have shown that single-fraction irradiation delivered to the whole brain in less than tenths of a second using FLASH radiotherapy (FLASH-RT), does not elicit neurocognitive deficits in mice. This observation has important clinical implications for the management of invasive and treatment-resistant brain tumors that involves relatively large irradiation volumes with high cytotoxic doses.

Experimental Design: Therefore, we aimed at simultaneously investigating the antitumor efficacy and neuroprotective benefits of FLASH-RT 1-month after exposure, using a well-characterized murine orthotopic glioblastoma model. As fractionated regimens of radiotherapy are the standard of care for glioblastoma treatment, we incorporated dose fractionation to simultaneously validate the neuroprotective effects and optimized tumor treatments with FLASH-RT.

Results: The capability of FLASH-RT to minimize the induction of radiation-induced brain toxicities has been attributed to the reduction of reactive oxygen species, casting some concern that this might translate to a possible loss of antitumor efficacy. Our study shows that FLASH and CONV-RT are isoefficient in delaying glioblastoma growth for all tested regimens. Furthermore, only FLASH-RT was found to significantly spare radiation-induced cognitive deficits in learning and memory in tumor-bearing animals after the delivery of large neurotoxic single dose or hypofractionated regimens.

Conclusions: The present results show that FLASH-RT delivered with hypofractionated regimens is able to spare the normal brain from radiation-induced toxicities without compromising tumor cure. This exciting capability provides an initial framework for future clinical applications of FLASH-RT.

See related commentary by Huang and Mendonca, p. 662

Introduction

Radiotherapy is a cornerstone of cancer treatment used in over 50% of patients with cancer in high-income countries (1, 2). However, its efficacy remains suboptimal in many radiation-resistant tumors such as glioblastoma, for which standard treatment consists of surgical resection followed by radiotherapy and concomitant temozolomide administration. Classical therapeutic protocols induce debilitating neurocognitive complications in a vast majority of patients, including impairments in learning and memory, attention, executive function, and variety of mood disorders (3–7), without efficiently eradicating the tumors. Therefore, any approach that could enhance normal tissue tolerance would dramatically improve the benefits of radiotherapy,

permitting increased doses to the tumor bed to achieve enhanced control (8–10). This fact has prompted efforts to develop truly innovative radiotherapy approaches able to eradicate tumors while sparing the normal brain from radiation-induced toxicities.

In this context, we have been the first to conceptualize and implement a novel modality of irradiation delivered at ultra-high dose rate (instantaneous dose rate > 10^6 Gy/s), named FLASH radiotherapy (FLASH-RT) using a low-energy electron (LEE) prototype linear accelerator (LINAC) eRT6/Oriatron (11, 12). We have recently shown that classical pathogenic patterns observed in normal tissues exposed to radiation delivered at conventional dose rates were not induced by single fractions of FLASH-RT (11–14), collective observations that we have since coined as the "FLASH effect." In the brain, long-term cognitive sparing was shown to be associated in part, by a lower production of reactive oxygen species (ROS), data obtained after the delivery of a single 10 Gy pulse over 1.8 μs (12, 14). While the capability of FLASH-RT versus conventional dose-rate radiotherapy (CONV-RT) to spare the normal brain from radiation-induced toxicities has been convincingly demonstrated, comprehensive studies exploring the efficacy of fractionated FLASH-RT on brain tumors were still lacking, but necessary to critically evaluate efficacy under a more clinically relevant scenario.

In this study, the LEE eRT6/Oriatron was set at its maximal electron current and the dose was delivered in a single—or maximum two pulses, which has proven to be optimal to achieve the FLASH effect (**Fig. 1**; ref. 15). These conditions were used to irradiate murine H454 glioblastoma tumors following orthotopic implantation of cells in the brain of Nude ($NU_{(Ico)}$-Foxn1^{nu}) mice. The choice of this orthotopic murine glioblastoma model, derived from genetically modified GFAP-HaRas^{V12};GFAP-CRE;GFAP-LUC;Trp53$^{Flox/WT}$ mice, was driven by its histopathologic resemblance to human glioblastoma,

[1]Laboratory of Radiation Oncology/DO/Radio-Oncology/CHUV, Lausanne University Hospital and University of Lausanne, Switzerland. [2]Department of Radiation Oncology, University of California, Irvine, California. [3]Institute of Radiation Physics/CHUV, Lausanne University Hospital, Switzerland.

Translational Relevance

With the capability to significantly preserve the normal brain from radiation-induced toxicities without compromising the efficacy of tumor treatments, irradiation at ultra-high dose rate referred as FLASH radiotherapy (FLASH-RT) provides a genuine therapeutic gain. Here we focus on the current shift toward hypofractionation in clinical practice and demonstrate that such an approach significantly maximizes the benefits of FLASH-RT in an orthotopic mouse model of glioblastoma. While the clinical implementation of FLASH-RT will require modifications to standard practice such as development of FLASH-capable accelerators as well as the adaptation of treatment regimens, there are many potential benefits including: (i) an improved management of radiation-resistant tumors for which dose escalation is necessary; (ii) an enhanced quality of life of cancer survivors by preventing debilitating side effects; (iii) minimized complications associated with organ motion, and (iv) an alleviated workload and reduced cost of cancer treatments.

including a highly infiltrative phenotype, anaplasia, and polymorphism (16). Furthermore, hypofractionated treatments were designed for tolerance based on projected tumor growth and animals' response to anesthesia, such that reliable clinical outcomes could be reproducibly evaluated. In every circumstance (single dose or fractionated; whole brain or hemibrain), we found that FLASH-RT was equally efficient as CONV-RT in delaying tumor growth. Significantly, only animals that received FLASH-RT, either as 10 Gy single dose or hypofractionated regimens (2×7 Gy and 3×10 Gy), did not exhibit neurocognitive decline. These results show that neurocognitive sparing can be achieved

with FLASH-fractionated regimens designed to approximate clinical treatment scenarios, without compromising tumor response. Moreover, these data again highlight a fundamental difference between the normal tissue and tumor response to FLASH-RT. While the "FLASH effect" remains to be elucidated at the mechanistic level, present data point to a unique opportunity to improve the radiotherapeutic management of brain cancer.

Materials and Methods

Animal experiments

Animal experiments were approved by Swiss (VD2920 and 3241) Ethics Committee for Animal Experimentation and performed within institutional guidelines. Female Nude ($NU_{(Ico)}$-$Foxn1^{nu}$) mice ($n = 8$–14 per group) were purchased from Charles River Laboratories at the age of 8 weeks.

Irradiation devices

Irradiation was performed using a prototype 6 MeV electron beam LINAC of type Oriatron 6e (eRT6; PMB Alcen), available at Lausanne University Hospital (Lausanne, Switzerland) and described previously (17). The eRT6/Oriatron beam is horizontal and not equipped with three-dimensional imaging capabilities, but with portal films for positioning, checking, and dosimetry. Physical dosimetry has been extensively described and published to ensure reproducible and reliable biological studies (12, 17–20). This LINAC is able to produce a pulsed electron beam at a mean dose rate ranging from 0.1 Gy/s (i.e., comparable with conventional dose rates used in radiotherapy) up to 7.8×10^6 Gy/s (at standard distance), corresponding to a dose, in each electron pulse, ranging from 0.01 up to 14 Gy. All FLASH irradiations were performed at an instantaneous dose rate above 1.8×10^6 Gy/s (i.e., the intrapulse dose rate). The beam parameters used throughout
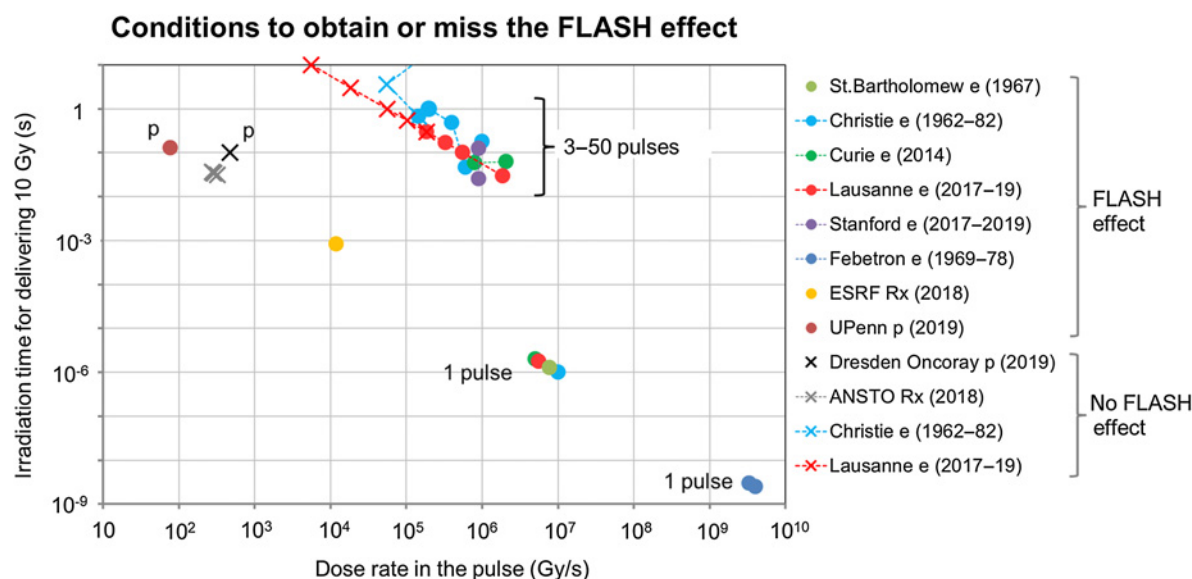
Figure 1.
Summary of the temporal dosimetry characteristics of the published experimental data describing the FLASH effect *in vivo* (11–14, 24, 27, 28, 34–37) or *in vitro* (38–42) (colored dots), those that have not been able to observe the FLASH effect (43, 44) (black, gray crosses) and the dose rate deescalation studies showing the range in which the FLASH effect is lost (colored crosses). The horizontal axis denotes the dose rate per pulse for electrons (e) and protons (p) or in a single stripe (as described in ref. 27) for synchrotron radiation (Rx). The vertical axis corresponds to the total irradiation time needed for delivering 10 Gy at the average dose rate quoted by the authors of the publications. Parameters for other dose values have been changed accordingly. Adapted from Bourhis and colleagues, 2019 (15).

Table 1. Irradiation parameters.

Delivery mode	Prescribed dose (Gy)	BED Brain $\alpha/\beta = 3$ (Gy)	BED Tumor $\alpha/\beta = 10$ (Gy)	Beam parameters							
				Graphite applicator type and size (mm)	Source-to-surface distance (mm)	Pulse repetition frequency (Hz)	Pulse width (μs)	Number of pulses	Treatment time (s)	Mean dose rate (Gy/s)	Instantaneous dose rate (Gy/s)
CONV	10	43.3	20.0	Circular Ø17	800	10	1.0	1,170–1,180	116.9–117.9	0.1	8.5×10^3
	14	79.3	33.6	Circular Ø17	803	10	1.0	1,467	146.6	0.1	9.5×10^3
	4 × 3.5	30.3	18.9	Circular Ø17	800	10	1.0	410	40.9	0.1	8.5×10^3
	2 × 7	46.7	23.8	Circular Ø17	800	10	1.0	822	82.1	0.1	8.5×10^3
	3 × 10	130	60.0	Circular Ø17	795	10	1.0	1,170–1,174	116.9–117.3	0.1	8.5×10^3
	25	233.3	87.5	Semicircular Ø17	745	10	1.0	2,620	261.9	0.1	9.5×10^3
FLASH	10	43.3	20.0	Circular Ø17	369–370	100	1.8	1	1.8×10^{-6}	5.6×10^6	5.6×10^6
	14	79.3	33.6	Circular Ø17	314–315	100	1.8	1	1.8×10^{-6}	7.8×10^6	7.8×10^6
	4 × 3.5	30.3	18.9	Circular Ø17	577	100	1.8	1	1.8×10^{-6}	1.9×10^6	1.9×10^6
	2 × 7	46.7	23.8	Circular Ø17	416–418	100	1.8	1	1.8×10^{-6}	3.9×10^6	3.9×10^6
	3 × 10	130	60.0	Circular Ø17	369–370	100	1.8	1	1.8×10^{-6}	5.6×10^6	5.6×10^6
	25	233.3	87.5	Semicircular Ø17	325	100	1.8	2	1.0×10^{-2}	2.5×10^3	6.9×10^6

this study are included in **Table 1**. The irradiation settings corresponding to the prescription dose for mouse irradiations were determined by surface dose measurements on a 30×30 cm²-solid water slab positioned behind a graphite applicator ($13.0 \times 13.0 \times 2.5$ cm³) with a 1.7-cm-diameter circular central aperture for whole brain irradiation (WBI) or semicircular aperture for hemibrain irradiation (HBI), as described previously (12, 20).

Tumor models and imaging

The H454 orthotopic murine glioblastoma model consists in injecting 500,000 H454 Luc+ murine glioblastoma cells (D. Hanahan, EPFL) in the right striatum of female Nude ($NU_{(Ico)}$-Foxn1^{nu}) mice with the coordinates: (AP: +1 mm; ML: +2 mm; DV: −3 mm). Cells were isolated from a GFAP-HaRas^{V12};GFAP-CRE;GFAP-LUC;Trp53$^{Flox/WT}$ genetically modified mouse model. Single dose or fractionated radiotherapy treatments (CONV or FLASH) started 3 days post-injection. Tumor development was assessed by bioluminescence (BLI) imaging the day of the first irradiation (normalized to 1) and weekly post-irradiation. Image acquisition was performed under isoflurane anesthesia using a Xenogen IVIS Lumina II (PerkinElmer, Inc.) and 10 minutes after an intraperitoneal injection of 15 mg/kg of luciferin and bioluminescence was quantified with Living Image Software (PerkinElmer, Inc.). The highly infiltrating features of H454 glioblastoma did not allow a postmortem correlation between semiquantitative BLI measurement and tumor volume. Tumor symptoms and survival were assessed.

The U87 orthotopic human glioblastoma model consists of injecting 50,000 U87 Luc+ human glioblastoma cells in the right striatum of Nude mice with the coordinates specified above. Tumor development was assessed by contrast-enhanced cone beam CT (CBCT) using iohexol contrast agent (200 μL of Accupaque 350 mg iodine per mL; GE Healthcare AG) right before imaging, providing for an accurate visualization of these bulkier tumors. Image acquisition was performed under isoflurane anesthesia using a small animal irradiator (X-rad 225Cx, Precision X-Ray) at 80 kV and 1.5 mA. Tumor volumes were measured from DICOM files with Osirix DICOM viewer (Pixmeo) and calculated with the formula of an ellipsoid volume: $V = \frac{4}{3} \times \pi \times L \times W \times H$.

Brain irradiations

All brain irradiations of tumor-bearing mice were performed under isoflurane anesthesia. For WBIs, the mouse was positioned directly behind the graphite applicator (in contact) with the head positioned in the 1.7-cm-diameter circular aperture in order to irradiate the whole encephalon region, while limiting the dose to the eyes, the mouth, and the rest of the body. For hemibrain irradiation, the head region was positioned in the 1.7-cm-diameter semicircular aperture to only expose the tumor-bearing brain hemisphere.

For WBIs, mice received 10 or 14 Gy single dose; daily fractionated doses of 4 × 3.5 Gy or 2 × 7 Gy; or 3 × 10 Gy spaced by 48 hours. For HBIs, a single dose of 25 Gy was delivered to the right hemisphere (see **Table 1** for irradiation parameters). For all regimen, FLASH and CONV irradiation modalities were compared.

Cognitive testing

To determine the effects of the different regimens of conventional and FLASH dose-rate radiotherapy on cognitive function, mice were subjected to behavioral testing 1 month after the first radiotherapy treatment. Mice bearing H454 orthotopic glioblastoma tumors were administered the novel object recognition (NOR) task (14) to assess memory skills associated to the cortex function (21, 22). Discrimination index (DI) were calculated as $\left(\frac{T_{novel}}{T_{total}} - \frac{T_{familiar}}{T_{total}}\right) \times 100$, where

T_{novel} is the time spent exploring the novel object, $T_{familiar}$ is the time spent exploring the familiar object, and T_{total} is the total time of exploration. Data analysis was conducted independently and blind and is presented as the average of all trials scored for each task. None of the treatment regimens resulted in observable skin toxicity or any other phenotypic differences that could have biased test scoring results.

Statistical analyses

Statistical analyses were carried out using GraphPad Prism (v8) software. P values were derived from the Mann–Whitney U test or log-rank test for survival studies. Results were expressed as mean values ± SD or mean values ± SEM, and all analyses considered a value of $P \leq 0.05$ to be statistically significant.

Results

As the number of groups investigating FLASH-RT steadily rise, the importance of carefully defining the critical beam parameters and other relevant conditions used to characterize the FLASH effect becomes increasingly important. In prior reports, these topics were discussed along with additional parameters such as instantaneous dose rate, duration of exposure and pulse repetition (among others), that now formally define the FLASH effect (15, 23). Here we have provided an updated version of the temporal dosimetry characteristics reported previously (15), that plot the duration of exposure versus the pulse dose rate from publications claiming to have produced—or not, the FLASH effect (**Fig. 1**). Importantly, we have collated and analyzed these data in detail to derive the optimized irradiation schedules selected for this study, and to help advance the field of FLASH-RT, we have provided a full characterization of all relevant FLASH beam parameters (**Table 1**). Dose-rate de-escalation studies using electrons have been conducted in the past (24) and more recently (12) and have identified a threshold of time of exposure and intrapulse dose rates that do not elicit the FLASH effect (colored cross **Fig. 1**).

Given the importance of carefully defining our beam parameters, the main focus of this study was not only to substantiate prior findings of normal tissue sparing in the FLASH irradiated brain but, to conclusively demonstrate that this new innovative irradiation modality was equally capable at controlling tumor growth compared with standard dose rate modalities. Second, and as alluded to above, we selected hypofractionated irradiation protocols to substantiate that both single and multifraction schedules were able to maintain the efficacy of tumor treatments while minimizing normal tissue toxicities.

To accomplish these objectives, we first used glioblastoma-bearing mice to investigate the antitumor efficacy of single doses of irradiation delivered with FLASH or CONV-RT. Nude mice implanted with H454 murine glioblastoma cells were given WBI using a single dose of 10 Gy, similarly to previously published normal tissue studies (12, 14), or 14 Gy with FLASH or CONV-RT, and tumor growth was quantified between nonirradiated controls and the irradiated groups as measured by bioluminescence over 4 weeks postirradiation. With 10 Gy, and for all time points, both conventional dose-rate irradiation (mean change in relative bioluminescence of 59.7 vs. 2436.0, $P < 0.01$ at 3-week time point) and FLASH-RT (mean fold change of 130.7 vs. 2436.0, $P < 0.0001$ at 3-week time point) showed a lower tumor burden compared with controls, whereas no difference in antitumor effects was observed between FLASH and conventional dose-rate irradiations ($P = 0.90$ at 3-week time point; **Fig. 2A**). Increasing the dose to 14 Gy single-dose WBI enhanced tumor growth delay with the two radiotherapy

modalities (mean fold change of 12.7 for 14 Gy CONV and 9.4 for 14 Gy FLASH vs. 1625 controls; $P < 0.001$ at 3-week time point), but without reaching tumor control (**Fig. 2B**). Furthermore, CONV-RT and FLASH-RT resulted in comparable survival rates (**Fig. 2D** and **E**), but limited efficacy.

Simultaneously, neurocognitive consequences of irradiation were investigated using the same animals with a NOR task. To avoid the potentially confounding impact of tumor progression on neurologic function, assessment of cortex-dependent recognition memory by NOR was evaluated at 4 weeks posttumor initiation, when cognition was not affected by the tumor *per se*. Nontreated animals show no drop in DI (39.3 ± 6.0, mean DI ± SEM, $n = 14$) depicting an absence of tumor-induced cognitive impairment (**Fig. 2G** and **H**). However, a drastic and significant drop in the DI was observed for the conventional dose-rate 10 Gy irradiated group compared with controls (18.0 ± 5.1 vs. 39.3 ± 6.0; $P = 0.021$). Remarkably, tumor-bearing animals subjected to FLASH-RT exhibited no such decrements and were statistically similar to controls (39.9 ± 3.6 vs. 39.3 ± 6.0; $P = 0.86$; **Fig. 2G**). Nevertheless after 14 Gy WBI, both CONV and FLASH irradiated groups showed a significant decrease in the DI (17.2 ± 5.3 vs. 50.4 ± 7.1 and 20.4 ± 8.3 vs. 50.4 ± 7.1; $P < 0.01$ and $P = 0.04$, respectively; **Fig. 2H**). While the underlying causes responsible for such a sharp dose-response curve require further investigation, our recent results in tumor-free animals indicates that the vascular (25) and glial (26) pathologic responses to irradiation are probably right shifted (i.e., toward higher doses) at ultra-high dose rates.

Altogether, these data show that a single dose of 10 Gy FLASH-RT is as efficient as CONV-RT to delay the growth of orthotopic glioblastoma but preserves mice cognitive skills. Nevertheless, dose escalation to 14 Gy FLASH, even if more efficacious against tumor, cannot be delivered without impairing the mice cognitive function and is not sufficient to reach tumor control. Therefore, we investigated the effect of 14 Gy delivered in 2 fractions of 7 Gy, 24 hours apart (**Fig. 2C**). Whereas 2 × 7 Gy antitumor efficacy was similar to a single dose of 14 Gy, ($P = 0.64$ for CONV and $P = 0.22$ for FLASH), neurocognitive testing showed a significant decrease in DI for animals treated with 2 × 7 Gy CONV as compared with the controls (11.7 ± 7.1 vs. 33.5 ± 4.3; $P = 0.01$), whereas FLASH irradiated animals depicted excellent performance 4 weeks posttreatment (49.4 ± 8.5 vs. 11.7; $P < 0.01$; **Fig. 2I**). No significant increase in survival was induced by this treatment regimen (**Fig. 3F**).

Next, to get closer to a dose per fraction used in clinics, we studied the effect of a 4 × 3.5 Gy daily fractionated regimen on H454 glioma-bearing animals (**Fig. 3A**, **C** and **E**). For all time points, both conventional dose-rate irradiation and FLASH-RT showed a similar but limited growth tumor delay (mean change of 95.1 and 89.8; $P < 0.001$ vs. control at 3-week time point), without any improvement of overall and survival (**Fig. 3A** and **C**). No cognitive impairment was observed with this protocol (**Fig. 3E**). Animals irradiated with CONV-RT or FLASH-RT showed equivalent performance as the nonirradiated animals on this task (22.1 ± 4.5 and 19.3 ± 8.4 vs. 33.5 ± 4.3; $P = 0.193$ and $P = 0.12$), showing no radiation-induced cognitive alteration. Thus, at low dose per fraction, there is no particular benefit of FLASH-RT over conventional dose rate, despite the fact that that the antitumor effect of FLASH-RT is maintained.

As none of the previous treatment regimens reached complete tumor control, nor improvement of overall survival, we investigated the effect of hypofractionated regimen of FLASH-RT on both H454 gliomas and normal tissue. Animals were exposed to 3 × 10 Gy spaced by 48 hours fractionated CONV-RT or FLASH-RT, corresponding to a biologically effective dose (BED) of 60 Gy (using an α/β
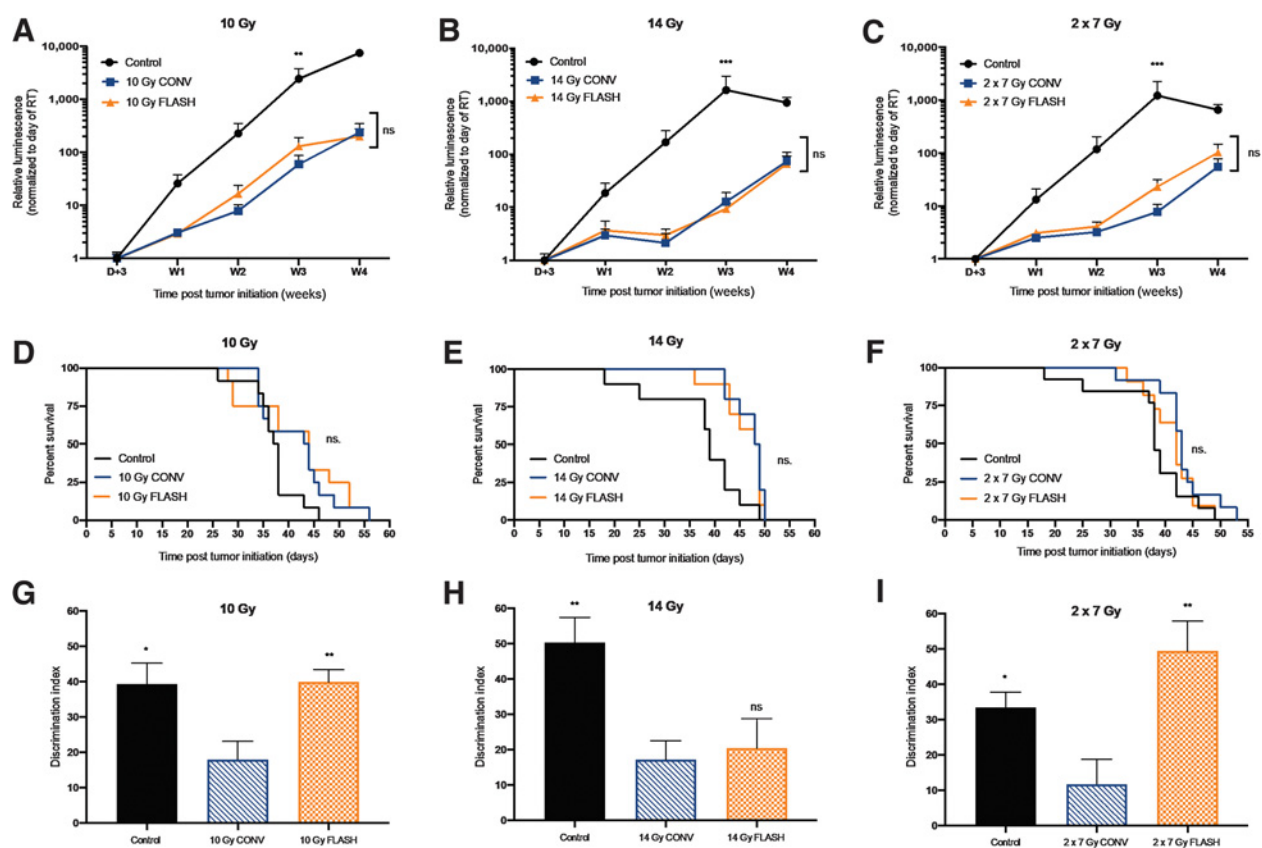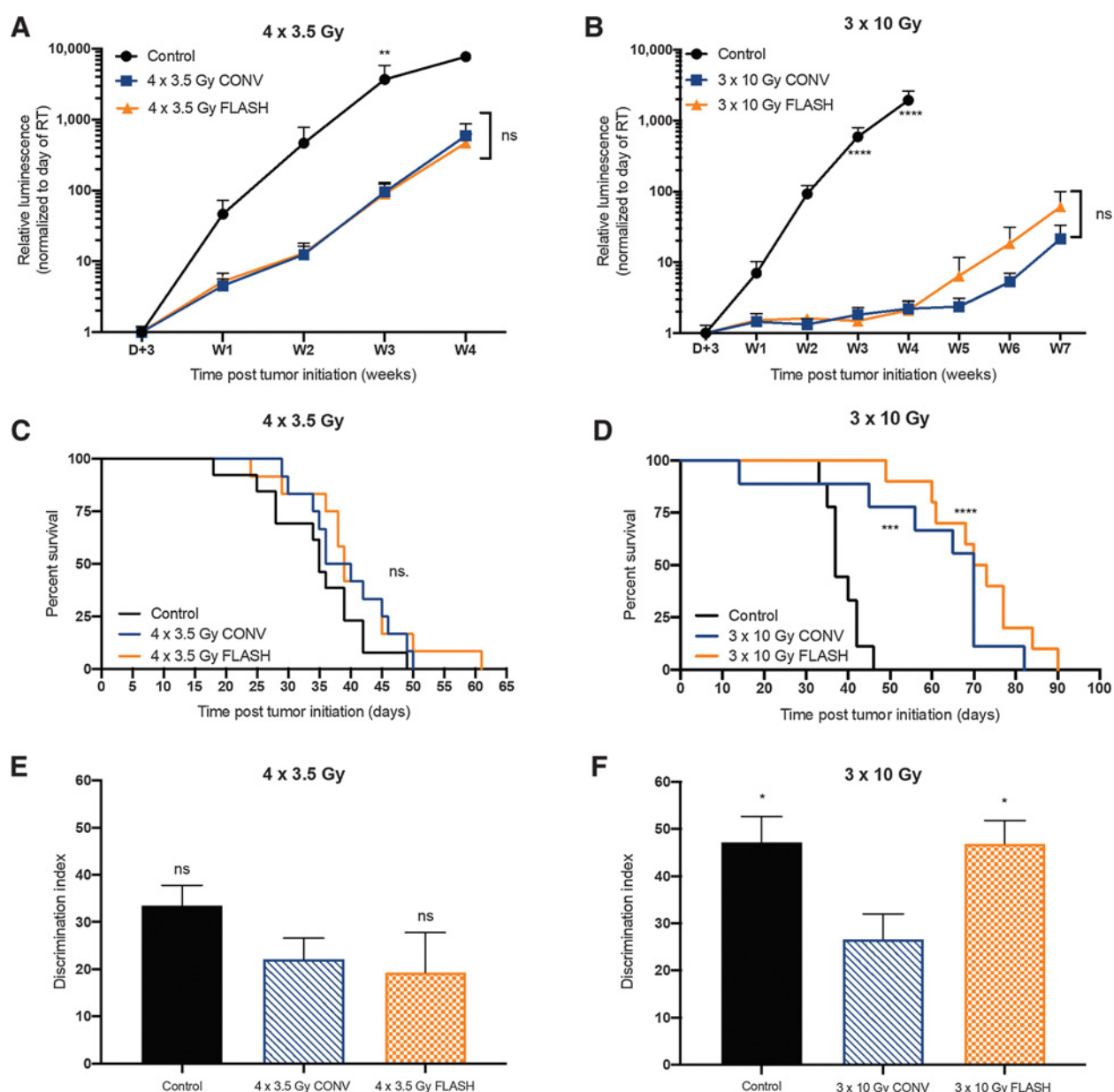
Figure 2.

Tumor growth delay of H454 orthotopic glioblastoma implanted in the striatum of female Nude mice measured by bioluminescence (**A–C**) treated with 0, 10 Gy (BED = 20 Gy), 14 Gy (BED = 33.6 Gy) single dose or 2 × 7 Gy (BED = 23.8 Gy) daily fractionated WBI delivered with FLASH or CONV-RT. Mean change in relative bioluminescence ± SEM, N = 10–12 animals per group. P values were derived from the Mann–Whitney U test: $**$, $P < 0.01$; $***$, $P < 0.001$ compared FLASH versus CONV group; ns, not significant. α/β ratio of 10 for BED calculation on the tumor. Survival curves of glioblastoma-bearing mice treated with 0, 10, or 14 Gy single dose or 2 × 7 Gy daily fractionated WBI with FLASH or CONV-RT (**D–F**). N = 10–12 animals per group. P values were derived from the log-rank test; compared FLASH versus CONV group. ns, not significant. Memory skills of glioblastoma-bearing mice treated with 0, 10 Gy (BED = 43.3 Gy), 14 Gy (BED = 79.3 Gy) single dose or 2 × 7 Gy (BED = 46.7 Gy) daily fractionated WBI delivered with FLASH or CONV-RT, evaluated by NOR test 4 weeks postimplantation (**G–I**). Mean DI ± SEM, N = 10–14 animals per group. P values were derived from the Mann–Whitney U test: $*$, $P < 0.05$; $**$, $P < 0.01$ compared Control and FLASH versus CONV group. ns, not significant. α/β ratio of 3 for BED calculation on the normal brain tissue.

of 10 for the tumor), a value close to the BED used in clinical care (BED of 72 Gy at 30 × 2 Gy; **Fig. 3B**, **D** and **F**). At 4-weeks after treatment, animals show significant tumor growth delay, demonstrating the efficacy of this regimen (mean change of 2.2 for CONV-RT and 2.1 for FLASH-RT vs. 1946.2 for controls, $P < 0.0001$). Once again, no difference in efficacy was observed between CONV and FLASH-RT ($P = 0.965$) using the murine glioblastoma cell line H454 (**Fig. 3B**) and confirmed using the human glioblastoma cell line U87 followed-up by CBCT imaging (Supplementary Fig. S1). Moreover, using H454, a significant increase in overall and median survival was observed after both treatments, with animals living up to 90 days post-treatment (**Fig. 3D**) while no relapse was observed in FLASH treated U87 animals over a period of 7 weeks (Supplementary Fig. S1A). Animals treated with 3 × 10 Gy FLASH-RT showed no cognition deficits compared with the control animals (46.9 ± 4.9 vs. 47.2 ± 5.4; $P > 0.999$), whereas CONV-RT induced a significant drop in the recognition memory skills (26.6 ± 5.3 vs. 47.2 ± 5.4; $P = 0.02$; **Fig. 3F**). These results show the possibility to increase the dose per fraction delivered with FLASH-RT to further increase the tumor growth delay without compromising the

neurocognition of irradiated animals, whereas CONV-RT drastically affects neurocognitive functions.

Finally, to mimic a conformal treatment, reach a complete tumor control and increase the overall survival of treated animals, we increased the dose delivered to the tumor site by irradiating only the tumor-bearing hemisphere, both improving the tumor targeting and normal tissue sparing. With this configuration, animals were exposed to 25 Gy HBI delivered with CONV or FLASH-RT (**Fig. 4**). Both CONV-RT and FLASH-RT showed a similar and significant improvement in tumor control compared with the nonirradiated animals, with a steady tumor burden up to 7 weeks postirradiation (2.3 and 2.7 mean change, respectively, vs. 1293 for controls, $P < 0.0001$; **Fig. 4A**). This improvement in tumor growth delay was coherent with an increase in overall and median survival in both treated groups, with animals free of tumors living up to 220 days post-irradiation (**Fig. 4B**). Nevertheless, with this irradiation configuration, both CONV or FLASH-RT groups showed comparable neurocognitive functions when compared with the nonirradiated animals (24.0 ± 8.9 and 21.1 ± 11.3, respectively, vs. 23.5 ± 11.6; $P > 0.70$), with large intragroup variations (**Fig. 4C**).
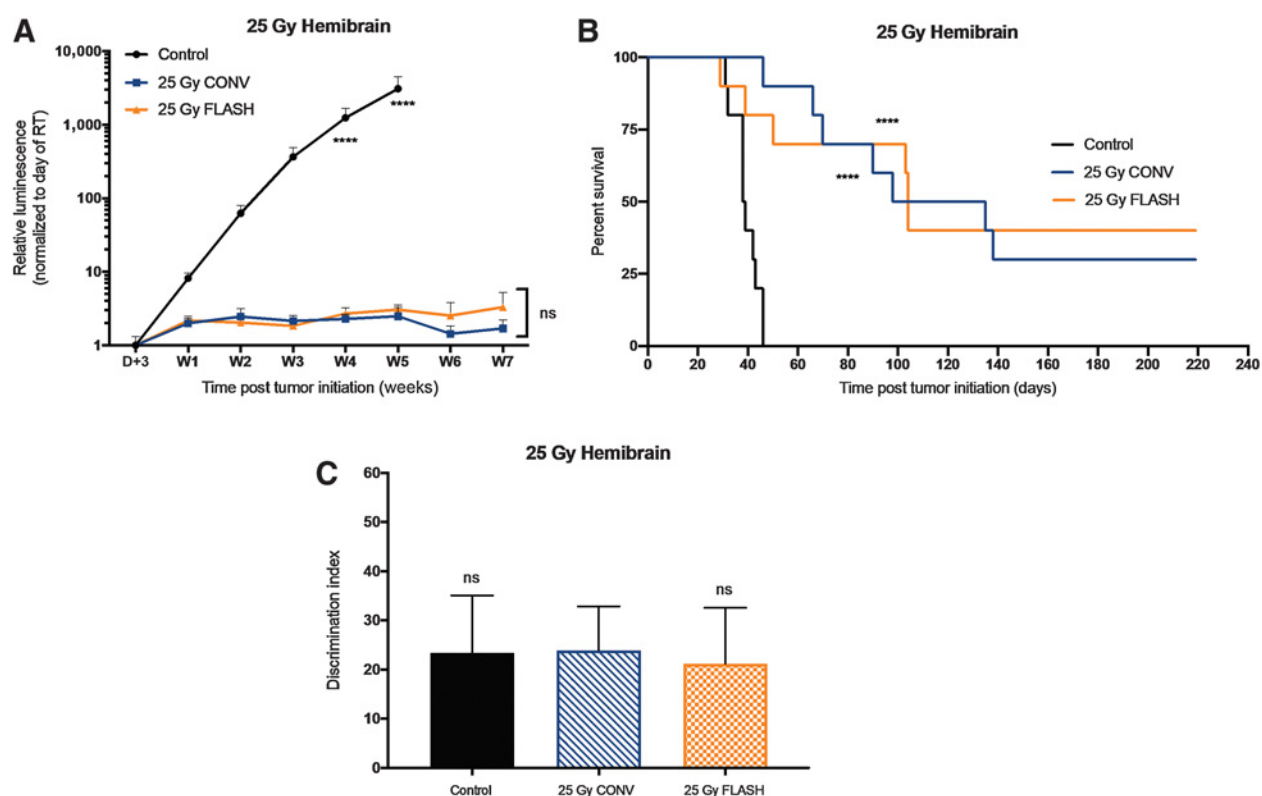
Figure 3.
Tumor growth delay of H454 orthotopic glioblastoma implanted in the striatum of female Nude mice treated with 0, 4×3.5 Gy (BED = 18.9 Gy) daily fractionated WBI; or 3×10 Gy (BED = 60 Gy) spaced by 48 hours WBI delivered with FLASH or CONV-RT (**A** and **B**). Mean change in relative bioluminescence $\pm$ SEM, $N = 9$–13 animals per group. P values were derived from the Mann–Whitney U test: **, $P < 0.01$; ***, $P < 0.001$; ****, $P < 0.0001$ compared FLASH versus CONV group; ns, not significant. α/β ratio of 10 for BED calculation on the tumor. Survival curves of glioblastoma-bearing mice treated with 0, 4×3.5 daily fractionated WBI; or 3×10 Gy spaced by 48 hours WBI delivered with FLASH or CONV-RT (**C** and **D**). $N = 9$–13 animals per group. P values were derived from the log-rank test. ***, $P < 0.001$; ****, $P < 0.0001$ versus control group; ns: not significant. Memory skills of glioblastoma-bearing mice treated with 0 Gy, 4×3.5 Gy (BED = 30.3 Gy) daily fractionated WBI; or 3×10 Gy (BED = 130 Gy) spaced by 48 hours WBI delivered with FLASH-RT or CONV-RT, evaluated by NOR test 4 weeks postimplantation (**E** and **F**). Mean DI $\pm$ SEM, $N = 8$–12 animals per group. P values were derived from the Mann–Whitney U test: *, $P < 0.05$; **, $P < 0.01$ compared with the CONV group. ns, not significant. α/β ratio of 3 for BED calculation on the normal brain tissue.

Discussion

The present results show in a single-murine glioblastoma model that FLASH-RT delivered with LEE with an instantaneous dose rate above 1.8×10^6 Gy/s is able to spare the normal brain from radiation-induced toxicities without compromising tumor cure.

Despite technical limitations, including limited study time points due to tumor aggressiveness and immunocompromised mouse models, data also establish an initial framework for future clinical applications and highlights the fact that hypofractionated protocols will likely provide the best option for maximizing the FLASH effect. These results also provide some baseline physics parameters for the
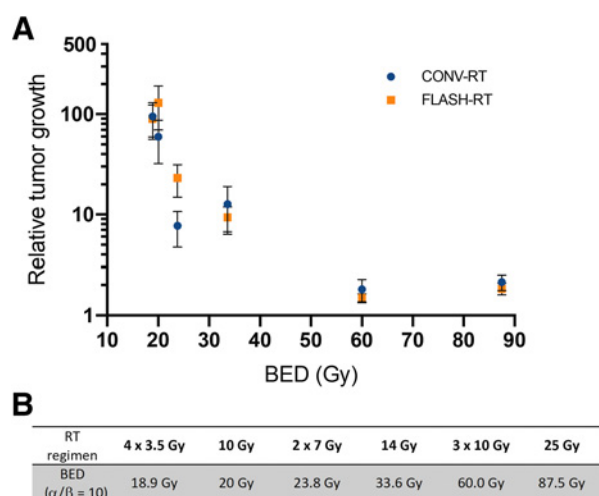
Figure 4.
Tumor growth delay of H454 orthotopic glioblastoma implanted in the striatum of female Nude mice measured by bioluminescence (**A**) treated with 25 Gy (BED = 233 Gy) single-dose HBI delivered with FLASH-RT or CONV-RT. Mean change in relative bioluminescence ± SEM, N = 9–10 animals per group. P values were derived from the Mann–Whitney U test: ****, P < 0.0001; ns, not significant. α/β ratio of 10 for BED calculation on the tumor. Survival curves of H454 glioblastoma-bearing mice (**B**) treated with 25 Gy single-dose HBI delivered with FLASH or CONV-RT. N = 10 animals per group. P values were derived from log-rank test: ***, P < 0.01; ****, P < 0.0001 compared with the control group. ns, not significant. Memory skills of glioblastoma-bearing mice treated with 25 Gy (BED = 87.5 Gy) single-dose HBI delivered with FLASH or CONV-RT, evaluated by NOR test 4 weeks postimplantation (**C**). Mean ± SEM, N = 9–10 animals per group. P values were derived from the Mann–Whitney U test: ns, not significant. α/β ratio of 3 for BED calculation on the normal brain tissue.

further exploration of normal tissue and tumor responses to FLASH irradiation. Moving forward, it will be critical to carefully validate the conditions required to observe the "FLASH effect" especially given that many research groups have entered the FLASH field, using various types of beams including protons, photons, and very high-energy electrons.

The definition and characterization of the optimal dose rate(s) able to produce the FLASH effect is an active topic of research in our group. While we first quoted the mean dose rate and reported thresholds for neurocognitive sparing above 100 Gy/s (12), we have since realized that this was an oversimplification. It should also be emphasized that in many of our past studies a single pulse was used, therefore, the mean dose rate was equal to the instantaneous dose rate. To help resolve any unnecessary confusion concerning FLASH-RT, we have recently documented the parametric characterization of the FLASH effect (**Fig. 1**; **Table 1**). In addition to the mean dose rate, additional parameters important for the FLASH effect include instantaneous dose rate, total duration of exposure, repetition rate (frequency), pulse dose, number of pulses, pulse width, total dose, and exposed volume. This comprehensive definition of FLASH-RT is required for scientific rigor, accuracy and reproducibility of not only current but, forthcoming datasets. These parameters are highly important to more completely understand the physical, physicochemical and biological processes involved in the FLASH effect. Such a formal characterization should

also be viewed as flexible rather than fixed, as new findings and discoveries will undoubtedly evolve and reshape our current views of FLASH-RT. Nonetheless, based upon the impressive functional outcomes reported here and previously (11–14, 27–29), clinical applications should be rapidly and pragmatically implemented (30). In this light, it remains important to point out that standard radiotherapy approaches currently use in clinics (intensity-modulated radiotherapy, stereotactic ablative radiotherapy, proton therapy, *etc.*) remain incompletely understood, pointing to the need to move more potentially efficacious treatments forward despite a thorough understanding of mechanism of action.

For instance, in the context of adult and especially pediatric patients with brain tumor, novel strategies are desperately needed for improving the therapeutic index of radiotherapy where progressive and debilitating normal tissue toxicities can severely compromise quality of life (3, 4). Given this backdrop, brain tumors were logical targets for the assessment of fractionated FLASH-RT efficacy since previous demonstrations of the FLASH effect in the brain were primarily done with single large doses and volumes (cm³). An orthotopic murine glioblastoma model was selected for its clinical relevance and feasibility to perform reliable and quantitative comparisons between the efficacy of FLASH-RT and CONV-RT. The best treatment regimen was subsequently implemented using a human orthotopic glioblastoma model and data confirmed that our findings could be extended to other

Figure 5.
Relative tumor growth delay of H454 orthotopic glioblastoma as a function of the BED delivered to the tumor with FLASH or CONV-RT, 3 weeks postirradiation (**A**). BED on the tumor was calculated with the following formula: $nd \times (1 + \frac{d}{\alpha/\beta})$, where n is the number of fractions, d is the dose per fraction, and the α/β ratio is set to 10 (**B**).

tumors including humans. In all tested regimens, the antitumor efficacies of CONV-RT and FLASH-RT were equivalent and increased with the BEDs (**Fig. 5A** and **B**). In addition, HBI results showed the benefits of a pseudoconformal approach combined with FLASH-RT, where higher FLASH doses could be used on smaller irradiated volumes to achieve tumor control. These data support the future implementation of state-of-the-art imaging to further optimize the advent of *bona-fide* conformal FLASH-RT. At the normal tissue level, only FLASH irradiated animals showed a preservation of cognition after hypofractionated and single-dose radiation exposures. Importantly, although variation in neurocognitive capability was observed in nonirradiated animals, sparing was achieved in FLASH-treated tumor-bearing animals after various treatment regimens including 10 Gy, 2×7 Gy and 3×10 Gy with respective BED of 43.3, 46.7, and 130 Gy (using an α/β ratio of 3 for normal brain) pointing to the promise of achieving similar normal tissue sparing in the clinic (BED on the normal brain around 100 Gy) following various hypofractionated regimens. Interestingly, we showed that the use of FLASH-RT was particularly beneficial when the toxicity triggered by conventional dose rate irradiation was substantial, highlighting the possibility to deliver larger doses per fraction with FLASH-RT.

To our knowledge, these findings are the first demonstration in an orthotopic tumor-bearing mouse model of an intervention capable of improving short-term neurocognitive outcome without compromising the radiation response of the tumor. In the presence of an aggressively growing tumor, neurocognitive testing is typically confounded, which highlights the need to conduct testing at relatively early times following irradiation, as opposed to tumor-free animals that can be evaluated at later postirradiation intervals. Nonetheless, our success at controlling both tumor growth and adverse cognitive outcomes highlights the potential promise of safely increasing the total dose for tumor cure, through ultra-high dose rate FLASH-RT. Because normal tissue tolerances currently limit the dose delivered to the tumor bed, the capability of FLASH to avoid typical normal tissue complications provides an exciting clinical prospect that promises to stimulate

further investigation in all disciplines of radiation oncology. Interestingly, the decreased production of ROS that we have previously described as one possible mechanism for normal brain protection (14) does not appear to impair tumor response, suggesting that additional tumor-specific mechanisms are involved.

The tumor cell line (H454) chosen in this study was isolated from the FVBN mouse strain that exhibits many behavioral abnormalities, rendering them nonsuitable for NOR testing. Therefore, we implanted the H454 cells in immunocompromised mice, which prohibits the investigation of immune cell contributions. Nevertheless, differences between tumor, normal cell metabolism and the microenvironment might provide some explanation for the FLASH effect. A recent report investigating FLASH and conventional dose rate irradiation has indicated the importance of oxygen tension in clonogenic survival assays (31), corroborating several past results (14, 32). Increased oxygen tension afforded by carbogen breathing was also found to negate the neurocognitive benefits of FLASH, again suggesting a role for oxygen and ROS in the FLASH effect (14). Moreover, tumor-related hypoxia in the context of treatment resistance remains to be investigated after CONV and FLASH-RT. Differences in redox metabolism between normal and tumor cells have also been proposed to account for some of the differential responses and have recently been proposed to model the FLASH effect (33). The capacities of normal cells to more efficiently regulate redox stress, including hydroperoxides and labile Fe, along with a decreased production of ROS could explain the differential effect observed between the tumor and normal tissue after FLASH-RT. While details remain to be validated by experimentation, multiple mechanisms are likely to operate simultaneously to elicit the FLASH effect and we among other labs are actively seeking to identify the best parameters to reproducibly and reliably optimize FLASH-RT.

In summary, while further in-depth experimentation is clearly needed to fully characterize the physical, physicochemical, and biological mechanisms of FLASH-RT, cautious implementation of this promising new cancer treatment seems increasingly plausible as the necessary technology becomes available.

Authors' Disclosures

Authors' Contributions

P. Montay-Gruel: Conceptualization, data curation, formal analysis, investigation, writing-original draft, writing-review and editing. **M.M. Acharya:** Conceptualization, data curation, investigation, writing-original draft, writing-review and editing. **P. Gonçalves Jorge:** Data curation, investigation. **B. Petit:** Data curation, investigation. **I.G. Petridis:** Data curation, investigation. **P. Fuchs:** Data curation, investigation. **R. Leavitt:** Data curation, investigation. **K. Petersson:** Data curation, investigation. **M. Gondré:** Data curation, investigation. **J. Ollivier:** Data curation, investigation. **R. Moeckli:** Supervision. **F. Bochud:** Supervision. **C. Bailat:** Supervision. **J. Bourhis:** Supervision, funding acquisition. **J.-F. Germond:** Formal analysis, supervision, validation. **C.L. Limoli:** Conceptualization, formal analysis, supervision, funding acquisition, validation, writing-original draft, writing-review and editing. **M.-C. Vozenin:** Conceptualization, resources, formal analysis, supervision, funding acquisition, validation, writing-original draft, project administration, writing-review and editing.

Acknowledgments

References

1. Delaney G, Jacob S, Featherstone C, Barton M. The role of radiotherapy in cancer treatment: estimating optimal utilization from a review of evidence-based clinical guidelines. Cancer 2005;104:1129–37.

2. Rosenblatt E, Izewska J, Anacak Y, Pynda Y, Scalliet P, Boniol M, et al. Radiotherapy capacity in European countries: an analysis of the Directory of Radiotherapy Centres (DIRAC) database. Lancet Oncol 2013;14:e79–86.

3. Meyers CA, Hess KR, Yung WKA, Levin VA. Cognitive function as a predictor of survival in patients with recurrent malignant glioma. J Clin Oncol 2000;18: 646–50.

4. Butler JM, Rapp SR, Shaw EG. Managing the cognitive effects of brain tumor radiation therapy. Curr Treat Options Oncol 2006;7:517–23.

5. Wellisch DK, Kaleita TA, Freeman D, Cloughesy T, Goldman J. Predicting major depression in brain tumor patients. Psychooncology 2002;11:230–8.

6. Alms WC, Franti TG, Shelton DP. Improved soil mixing and delivery system for a storm runoff simulator. Appl Eng Agric 2011;27:579–86.

7. Caceres LG, Cid MP, Uran SL, Zorrilla Zubilete MA, Salvatierra NA, Guelman LR. Pharmacological alterations that could underlie radiation-induced changes in associative memory and anxiety. Pharmacol Biochem Behav 2013;111:37–43.

8. Bentzen SM. Preventing or reducing late side effects of radiation therapy: radiobiology meets molecular pathology. Nat Rev Cancer 2006;6:702–13.

9. Begg AC, Stewart FA, Vens C. Strategies to improve radiotherapy with targeted drugs. Nat Rev Cancer 2011;11:239–53.

10. Yarnold J, Vozenin Brotons MC. Pathogenetic mechanisms in radiation fibrosis. Radiother Oncol 2010;97:149–61.

11. Favaudon V, Caplier L, Monceau V, Pouzoulet F, Sayarath M, Fouillade C, et al. Ultrahigh dose-rate FLASH irradiation increases the differential response between normal and tumor tissue in mice. Sci Transl Med 2014;6:245ra93.

12. Montay-Gruel P, Petersson K, Jaccard M, Boivin G, Germond JF, Petit B, et al. Irradiation in a flash: unique sparing of memory in mice after whole brain irradiation with dose rates above 100 Gy/s. Radiother Oncol 2017;124: 365–9.

13. Vozenin M-C, De Fornel P, Petersson K, Favaudon V, Jaccard M, Germond J-F, et al. The advantage of Flash radiotherapy confirmed in mini-pig and cat-cancer patients. Clin Cancer Res 2019;25:35–42.

14. Montay-Gruel P, Acharya MM, Petersson K, Alikhani L, Yakkala C, Allen BD, et al. Long-term neurocognitive benefits of FLASH radiotherapy driven by reduced reactive oxygen species. Proc Natl Acad Sci U S A 2019;166:10943–51.

15. Bourhis J, Montay-Gruel P, Gonçalves Jorge P, Bailat C, Petit B, Ollivier J, et al. Clinical translation of FLASH radiotherapy: why and how? Radiother Oncol 2019;139:11–7.

16. Shchors K, Massaras A, Hanahan D. Dual targeting of the autophagic regulatory circuitry in gliomas with repurposed drugs elicits cell-lethal autophagy and therapeutic benefit. Cancer Cell 2015;28:456–71.

17. Jaccard M, Durán MT, Petersson K, Germond JF, Liger P, Vozenin MC, et al. High dose-per-pulse electron beam dosimetry: commissioning of the Oriatron eRT6 prototype linear accelerator for preclinical use: commissioning. Med Phys 2018;45:863–74.

18. Jaccard M, Petersson K, Buchillier T, Germond JF, Durán MT, Vozenin MC, et al. High dose-per-pulse electron beam dosimetry: usability and dose-rate independence of EBT3 Gafchromic films: usability. Med Phys 2017;44:725–35.

19. Petersson K, Jaccard M, Germond JF, Buchillier T, Bochud F, Bourhis J, et al. High dose-per-pulse electron beam dosimetry -A model to correct for the ion recombination in the advanced markus ionization chamber. Med Phys 2017;44: 1157–67.

20. Jorge PG, Jaccard M, Petersson K, Gondré M, Durán MT, Desorgher L, et al. Dosimetric and preparation procedures for irradiating biological models with pulsed electron beam at ultra-high dose-rate. Radiother Oncol 2019;139:34–9.

21. Barker GRI, Warburton EC. When is the hippocampus involved in recognition memory? J Neurosci 2011;31:10721–31.

22. Barker GRI, Bird F, Alexander V, Warburton EC. Recognition memory for objects, place, and temporal order: a disconnection analysis of the role of the medial prefrontal cortex and perirhinal cortex. J Neurosci 2007;27: 2948–57.

23. Wilson JD, Hammond EM, Higgins GS, Petersson K. Ultra-high dose rate (FLASH) radiotherapy: silver bullet or fool's gold. Front Oncol 2020;9:1563.

24. Hendry JH, Moore JV, Hodgson BW, Keene JP. The constant low oxygen concentration in all the target cells for mouse tail radionecrosis. Radiat Res 1982; 92:172–81.

25. Allen BD, Acharya MM, Montay-Gruel P, Jorge Goncalves P, Bailat C, Petit B, et al. Maintenance of tight junction integrity in the absence of vascular dilation in the brain of mice exposed to ultra-high-dose-rate FLASH irradiation. Radiat Res 2020.

26. Montay-Gruel P, Markarian M, Allen BD, Baddour JD, Giedzinski E, Jorge Goncalves P, et al. Ultra-high-dose-rate FLASH irradiation limits reactive gliosis in the brain. Radiat Res 2020.

27. Montay-Gruel P, Bouchet A, Jaccard M, Patin D, Serduc R, Aim W, et al. X-rays can trigger the FLASH effect: ultra-high dose-rate synchrotron light source prevents normal brain injury after whole brain irradiation in mice. Radiother Oncol 2018;129:582–8.

28. Simmons DA, Lartey FM, Schüler E, Rafat M, King G, Kim A, et al. Reduced cognitive deficits after FLASH irradiation of whole mouse brain are associated with less hippocampal dendritic spine loss and neuroinflammation. Radiother Oncol 2019;139:4–10.

29. Bourhis J, Sozzi WJ, Jorge PG, Gaide O, Bailat C, Duclos F, et al. Treatment of a first patient with FLASH-radiotherapy. Radiother Oncol 2019;139:18–22.

30. Harrington KJ. Ultrahigh dose-rate radiotherapy: next steps for FLASH-RT. Clin Cancer Res 2019;25:3–5.

31. Adrian G, Konradsson E, Lempart M, Bäck S, Ceberg C, Petersson K. The FLASH effect depends on oxygen concentration. Br J Radiol 2020;93: 20190702.

32. Vozenin MC, Hendry JH, Limoli CL. Biological benefits of ultra-high dose-rate FLASH radiotherapy: sleeping beauty awoken. Clin Oncol 2019;31:407–15.

33. Spitz DR, Buettner GR, Petronek MS, St-Aubin JJ, Flynn RT, Waldron TJ, et al. An integrated physico-chemical approach for explaining the differential impact of FLASH versus conventional dose rate irradiation on cancer and normal tissue responses. Radiother Oncol 2019;139:23–7.

34. Levy K, Natarajan S, Wang J, Chow S, Eggold J, Loo P, et al. FLASH irradiation enhances the therapeutic index of abdominal radiotherapy in mice. bioRxiv 2019.

35. Loo BW, Schuler E, Lartey FM, Rafat M, King GJ, Trovati S, et al. (P003) delivery of ultra-rapid flash radiation therapy and demonstration of normal tissue sparing after abdominal irradiation of mice. Int J Radiat Oncol 2017; 98:E16.

36. Schüler E, Trovati S, King G, Lartey F, Rafat M, Villegas M, et al. Experimental platform for ultra-high dose rate FLASH irradiation of small animals using a clinical linear accelerator. Int J Radiat Oncol Biol Phys 2017;97:195–203.

37. Diffenderfer ES, Verginadis II, Kim MM, Shoniyozov K, Velalopoulou A, Goia D, et al. Design, implementation and *in vivo* validation of a novel proton FLASH radiotherapy system. Int J Radiat Oncol Biol Phys 2020;106:440–8.

38. Epp ER, Weiss H, Djordjevic B, Santomasso A. The radiosensitivity of cultured mammalian cells exposed to single high intensity pulses of electrons in various concentrations of oxygen. Radiat Res 1972;52:324.

39. Town CD. Radiobiology. Effect of high dose rates on survival of mammalian cells. Nature 1967;215:847–8.

40. Michaels HB, Epp ER, Ling CC, Peterson EC. Oxygen sensitization of CHO cells at ultrahigh dose rates: prelude to oxygen diffusion studies. Radiat Res 1978;76: 510–21.

41. Berry RJ, Hall EJ, Forster DW, Storr TH, Goodman MJ. Survival of mammalian cells exposed to x rays at ultra-high dose-rates. Br J Radiol 1969;42:102–7.

42. Nias AH, Swallow AJ, Keene JP, Hodgson BW. Effects of pulses of radiation on the survival of mammalian cells. Br J Radiol 1969;42:553.

43. Beyreuther E, Karsch L, Laschinsky L, Leßmann E, Naumburger D, Oppelt M, et al. Radiobiological response to ultra-short pulsed megavoltage electron beams of ultra-high pulse dose rate. Int J Radiat Biol 2015;91:643–52.

44. Smyth LML, Donoghue JF, Ventura JA, Livingstone J, Bailey T, Day LRJ, et al. Comparative toxicity of synchrotron and conventional radiation therapy based on total and partial body irradiation in a murine model. Sci Rep 2018;8: 12044.